Hindawi
Mathematical Problems in Engineering
Volume 2021, Article ID 6626411, 9 pages
https://doi.org/10.1155/2021/6626411

Research Article

Three-Dimensional Rotating Flow of MHD Jeffrey Fluid Flow between Two Parallel Plates with Impact of Hall Current

Mehreen Fiza,[1] Abdelaziz Alsubie,[2] Hakeem Ullah,[1] Nawaf N. Hamadneh,[2] Saeed Islam,[1] and Ilyas Khan[3,4]

[1]*Department of Mathematics, Abdul Wali Khan University, Mardan, Pakistan*
[2]*Department of Basic Sciences, College of Science and Theoretical Studies, Saudi Electronic University, Riyadh 11673, Saudi Arabia*
[3]*Department of Mathematics and Statistics, Ton Duc Thang University, Ho Chi Minh City 72915, Vietnam*
[4]*Department of Mathematics, College of Science Al-Zulfi, Majmaah University, Al-Majmaah 11952, Saudi Arabia*

Correspondence should be addressed to Hakeem Ullah; hakeemullah1@gmail.com and Ilyas Khan; i.said@mu.edu.sa

Received 7 December 2020; Revised 19 January 2021; Accepted 8 March 2021; Published 19 March 2021

Academic Editor: Ahmad Zeeshan

This article deals with three-dimensional non-Newtonian Jeffrey fluid in rotating frame in the presence of magnetic field. The flow is studied in the application of Hall current, where the flow is assumed in steady states. The upper plate is considered fixed, and the lower is kept stretched. The fundamental equations are transformed into a set of ordinary differential equations (ODEs). A homotopy technique is practiced for a solution. The variation in the skin friction and its effects on the velocity fields have been examined numerically. The effects of physical parameters are discussed in various plots.

1. Introduction

The rotation of fluid exists in nature due to the fact that the fluid particles rotate internally and rises with fluid movement. Due to engineering and industrial applications, the scientist considers the rotational fluid coupled with various features. Rotational fluids have many applications in engineering. Taylor and Geoffrey introduced the motion of viscous fluid in the rotating system [1]. The detailed study of fluid in rotating system is done by Greenspan [2] and Goodman [3]. The effects of MHD in a rotating system and stretched and porous mediums have been studied by Attia and Kotb [4], Borkakoti and Bharali [5], and Vajravelu and Kumar [6]. This work has been magnified along with the temperature effects by Mehmood and Ali [7], Das et al. [8], and Tauseef et al. [9].

The non-Newtonian fluid is used in many industry and technology appliances. Hayat et al. studied the non-Newtonian fluid in a rotating frame, considering the effects of MHD for micropolar nanofluids [11, 12]. Jeffrey's model was presented by Jeffrey as a subclass of non-Newtonian fluid and studied with convection term [13, 14].

Most of the physical problems are nonlinear and have rare exact solutions. The numerical methods (NMs) and analytical methods (AMs) are used to get the results. The NMs required discretization techniques which can affect the results. Among the AMs, HAM proposed by Liao is the most powerful and fast convergent [15–19]. Hall introduced Hall current and proves that, in case of strong magnetic field, the Hall current effects cannot be ignored [20]. Similar other interesting studies are provided in [21–32] for different fluid models. This article aims to elaborate the non-Newtonian nanofluid in the rotating frame with Hall effect. Hall effect is produced due to the potential difference across an electrical conductor when a magnetic field is acting in a direction vertical to that of the flow of current. So, for this aim, Jeffrey fluid flow is considered. For the proposed model, HAM is used.

2. Problem Formulation

Assume the Jeffrey fluid between two parallel plates having d separation. The plate and fluid rotate about y axis with Ω. The lower plate is stretched by two opposite and equal forces. A uniform magnetic field B_0 is applied perpendicularly with a steady-state condition (Figure 1).

The fundamental identities are

$$\widehat{u}_x + \widehat{v}_y + \widehat{w}_z = 0, \tag{1}$$

$$\begin{aligned}\rho\left(u\widehat{u}_x + v\widehat{u}_y + 2w\Omega\right) = {} & -\widehat{p}_x + \frac{\mu}{1} + \gamma_1\left(\widehat{u}_{xx} + \widehat{u}_{yy}\right) - \left(\frac{\sigma B_0^2}{1} + m^2\right)(u + mw) + \left(\frac{\mu\gamma_2}{1+\gamma_1}\right) \\ & \cdot \left[\left(2\widehat{u}_x\widehat{u}_{xx} + 2\widehat{v}_x\widehat{u}_{xy}\right) + u\left(\widehat{u}_{xxx} + \widehat{u}_{xyy}\right) + v\left(\widehat{u}_{xxy} + \widehat{u}_{yyy}\right) + \widehat{u}_y \cdot \left(\widehat{v}_{xx} + \widehat{u}_{yx}\right) + \left(\widehat{u}_{yy} + \widehat{v}_{xy}\right)\widehat{v}_y\right],\end{aligned} \tag{2}$$

$$\begin{aligned}\rho\left(u\widehat{v}_x + v\widehat{v}_y\right) = {} & -\widehat{p}_y + \left(\frac{\mu}{1} + \gamma_1\right)\left(\widehat{v}_{xx} + \widehat{v}_{yy}\right) + \left(\frac{\mu\gamma_2}{1} + \gamma_1\right) \\ & \cdot \left[\left(2\widehat{v}_y\widehat{v}_{yy} + 2\widehat{u}_y\widehat{v}_{yx}\right) + \left(\widehat{v}_{xxx} + \widehat{v}_{xyy}\right)u + \left(\widehat{v}_{xxy} + \widehat{v}_{xyy}\right)v + \left(\widehat{u}_{xy} + \widehat{v}_{xx}\right)\widehat{u}_x + \left(\widehat{u}_{yy} + \widehat{v}_{xy}\right)\widehat{v}_y\right],\end{aligned} \tag{3}$$

$$\begin{aligned}\rho\left(u\widehat{w}_x + v\widehat{w}_y - 2\Omega u\right) = {} & \left(\frac{\mu}{1} + \gamma_1\right)\left(\widehat{w}_{xx} + \widehat{w}_{yy}\right) - \left(\frac{\sigma B_0^2}{1} + m^2\right)(mu - w) \\ & + \left(\frac{\mu\gamma_2}{1} + \gamma_1\right)\left[\left(\widehat{w}_{yyy} + \widehat{w}_{xxy}\right)v + \widehat{w}_{xy}\widehat{u}_y + \widehat{u}_x\widehat{w}_{xx} + u\left(\widehat{w}_{xxx} + \widehat{w}_{xyy}\right)\right].\end{aligned} \tag{4}$$

The BCs are

$$\begin{aligned}\widehat{u}(0) &= ax, \\ \widehat{v}(0) &= 0 = \widehat{w}(0), \\ \widehat{u}(d) &= \widehat{v}(d) = \widehat{w}(d) = 0.\end{aligned} \tag{5}$$

The similarity transformation used is

$$\begin{aligned}\widehat{u} &= axf'(\eta), \\ \widehat{v} &= -a\,df(\eta), \\ \widehat{w} &= axg(\eta), \\ \eta &= \frac{y}{d}.\end{aligned} \tag{6}$$

Using equation (6) in (1)–(4), we get

$$f'''' + (1+\gamma_1)\left(R\left(ff''' - f'f''\right)\right) - 2Krg' = \left(\frac{M}{1} + m^2\right)(f'' + mg') + \beta\left(2f''f''' - ff'''' - f'f'''''\right), \tag{7}$$

$$g'' + (1+\gamma_1)R(fg' - gf') + 2Krf' = \left(\frac{M}{1} + m^2\right)(g - mf') + \beta\left(fg''' - g'f''\right). \tag{8}$$

Substituting equation (8) in (7), we get

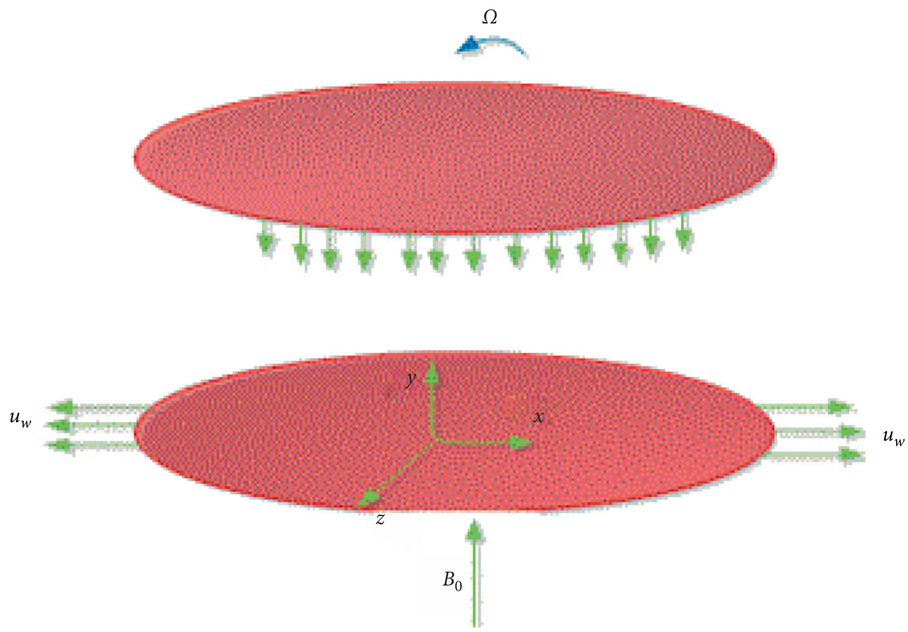

Figure 1: Geometrical structure of the flow problem.

$$\begin{aligned} f(0) &= 0,\\ f'(0) &= 1,\\ g(0) &= 0,\\ f(1) &= 0,\\ f'(1) &= 0,\\ g(1) &= 0, \end{aligned} \tag{9}$$

where

$$\begin{aligned} Kr &= \frac{2\Omega d^2}{\nu},\\ R &= \frac{a d^2}{\nu},\\ M &= \frac{\sigma B_0^2 d^2}{\rho v},\\ \beta &= a\gamma_2. \end{aligned} \tag{10}$$

C_f is given as

$$c_f = \frac{(\mu/(1+\gamma_1))\left[\left(\partial^2 v/\partial x^2\right) + \left(\partial^2 v/\partial y^2\right) + \gamma_2\left(u\left(\partial^2 u/\partial x\,\partial y\right) + v\left(\partial^2 v/\partial x\,\partial y\right) + u\left(\partial^2 v/\partial x^2\right) + v\left(\partial^2 u/\partial y^2\right)\right)\right]_{y=0}}{\rho u_w^2}. \tag{11}$$

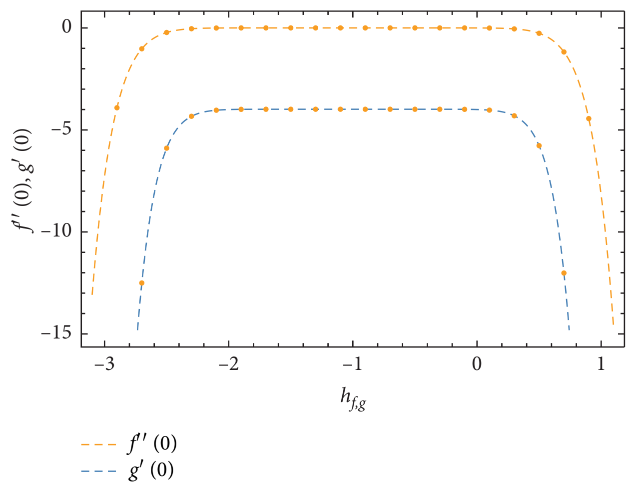

FIGURE 2: Combined h curves of function and velocity, at the 15th-order approximation.

The dimensionless form of c_f is

$$c_f\sqrt{\mathrm{Re}_x} = (1+\gamma_1)^{-1}\left(f''(0) + \beta f''(0)\right). \tag{12}$$

3. Solution Procedure

HAM was introduced by Liao. Let Ψ_1, Ψ_2 are two continuous functions defined on topological spaces $\tilde{X}$, $\tilde{Y}$, then

$$\psi\colon \hat{\tilde{X}} \times [0,1] \longrightarrow \hat{\tilde{Y}}, \tag{13}$$

such that $\tilde{x} \in \tilde{X}$:

$$\begin{aligned}\psi(0) &= \Psi_1,\\ \psi(1) &= \Psi_2.\end{aligned} \tag{14}$$

The initial guesses are

TABLE 1: Convergence table of HAM up to the 25th-order approximations when $R = \beta = \gamma_1 = m = M = 0.01$.

Order of approximation	$f''(0)$	$g'(0)$
1	3.18886	0.2207921
3	3.17650	0.2387064
6	3.17584	0.2396453
11	3.17583	0.2396677
15	3.17583	0.2396682
20	3.17583	0.2396682

$$\begin{aligned}f_0 &= \eta^3 - 2\eta^3 + \eta,\\ g_0 &= 0.\end{aligned} \tag{15}$$

The linear terms are

$$\begin{aligned}L_l(f) &= f_{\eta\eta\eta\eta},\\ L_l(g) &= g_{\eta\eta},\end{aligned} \tag{16}$$

with differential operator

$$\begin{aligned}L_l\left(D_1 + D_2\eta + D_3\eta^2 + D_4\eta^3\right) &= 0,\\ L_{ll}\left(D_5 + D_6\eta\right) &= 0,\end{aligned} \tag{17}$$

where D_n represents arbitrary constants, where $n = 1, 2, 3, \ldots, 6$.

3.1. Zeroth-Order Problem. Express $q \in [0 \;\; 1]$ as an embedding parameter with h_f and h_g, where $h \neq 0$. Then,

$$\begin{aligned}(1-q)L_i\left(\tilde{f}(\eta,q) - \tilde{f}_0(\eta)\right) &= p h_f \mathrm{N}_f\left(\hat{f},\hat{g}\right),\\ (1-q)L_g\left(\tilde{g}. - \tilde{g}_0(\eta)\right) &= p h_g \mathrm{N}_g\left(\tilde{f},\tilde{g}\right).\end{aligned} \tag{18}$$

The BCs are

$$\begin{aligned}&\tilde{f}(o,q). = \tilde{g}_{..}(o,q). = \tilde{f}'(o,q.) = 0,\\ &\tilde{f}(1,q.) = \tilde{g}(1,q) = \tilde{f}'(1,q) = 0,\\ &\mathrm{N}_l = \hat{f}_{\eta\eta\eta\eta} + (1+\gamma_1)\left(R\left(\hat{f}_{\eta\eta\eta}\hat{f} - \hat{f}_{\eta\eta}\hat{f}_\eta\right) - 2kr\hat{g}_\eta(\eta;q) - \frac{M}{1+m^2}\left(\hat{f}_{\eta\eta} + m\hat{g}_\eta(\eta;q)\right)\right)\\ &\qquad + \beta\left(2\hat{f}_{\eta\eta}\hat{f}_{\eta\eta\eta} - \hat{f}\hat{f}_{\eta\eta\eta\eta} - \hat{f}_\eta\hat{f}_{\eta\eta\eta\eta\eta}\right),\\ &\mathrm{N}_{ll} = \hat{g}_{\eta\eta} + (1+\gamma_1)R\left(\hat{f}\hat{g}_\eta - \hat{g}\hat{f}_\eta\right) + 2kr\hat{f}_\eta + \left(\frac{M}{1} + m^2\right)\left(m\hat{f}_\eta - \hat{g}\right) + \beta\left(\hat{g}_\eta\hat{f}_{\eta\eta} - \hat{g}_{\eta\eta\eta}\hat{f}\right),\end{aligned} \tag{19}$$

where

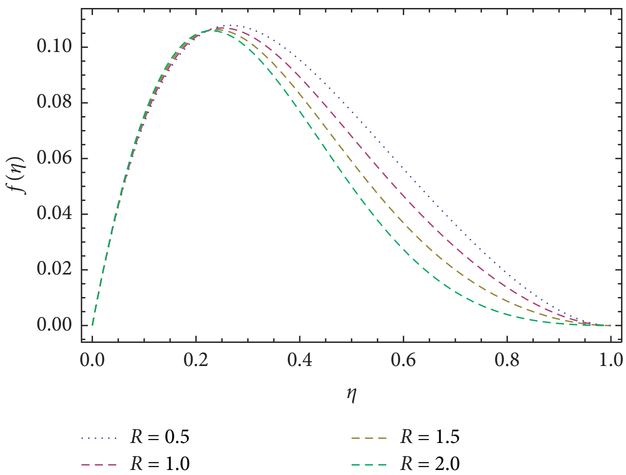

FIGURE 3: Effect of R on $f(\eta)$ when $m = 0.5, \gamma_1 = 0.7, M = 1, \beta = 0.4,$ and $kr = 0.6$.

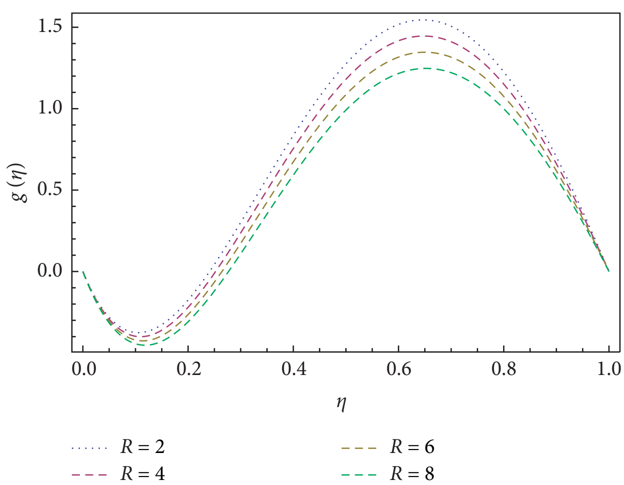

FIGURE 4: Effect of R on $g(\eta)$when $m = 0.5, \gamma_1 = 0.7, M = 1, \beta = 0.4,$ and $kr = 0.6$.

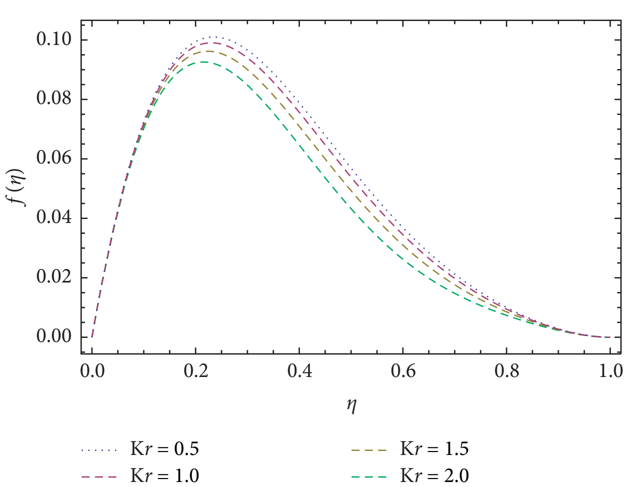

FIGURE 5: Effect of kr on $f(\eta)$ when $m = \gamma_1 = 0.8, M = 0.4, R = 1,$ and $\beta = 0.4$.

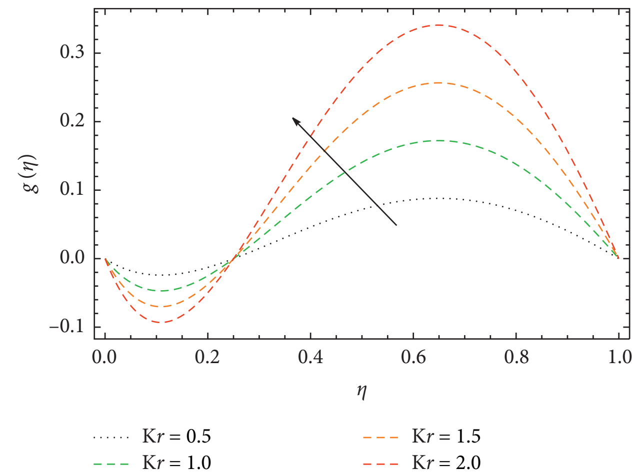

FIGURE 6: Effect ofkr on $g(\eta)$ when $m = \gamma_1 = 0.8, M = 0.4, R = 1,$ and $\beta = 0.4$.

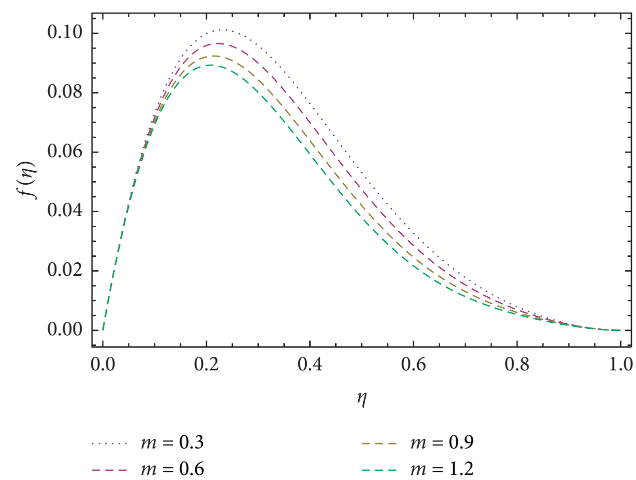

FIGURE 7: Effect of m on$f(\eta)$ when $R = 1, \gamma_1 = 0.7, \beta = 0.4, M = 1,$ and $kr = 0.6$.

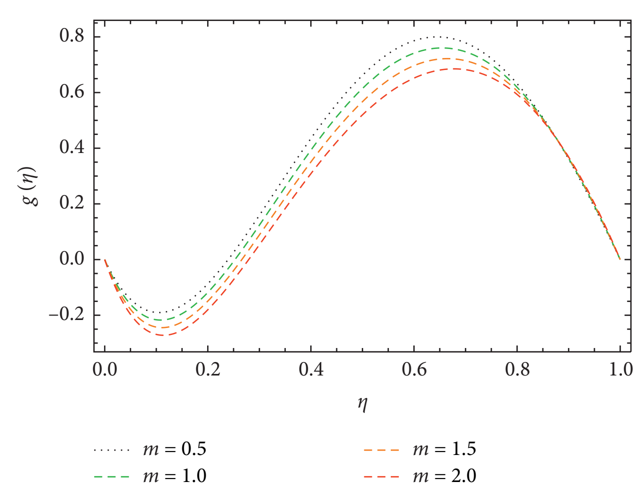

FIGURE 8: Effect of m on $g(\eta)$ when $R = 1, \gamma_1 = 0.7, \beta = 0.4, M = 1,$ and $kr = 0.6$.

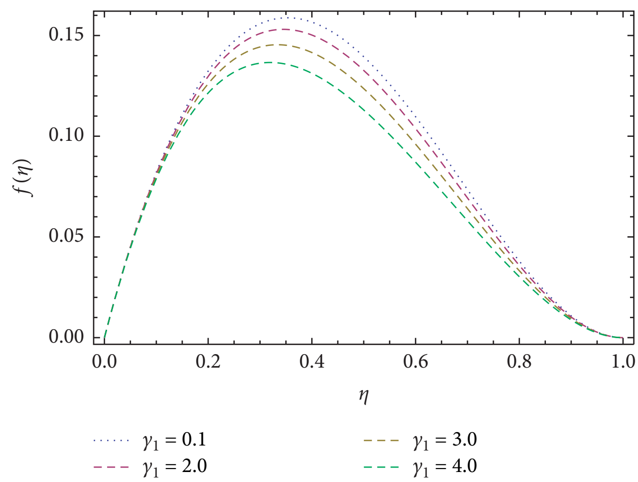

FIGURE 9: Effect of γ_1 on $f(\eta)$ when.$R = 0.1, m = 0.8, \beta = 0.4$, and $M = kr = 1$.

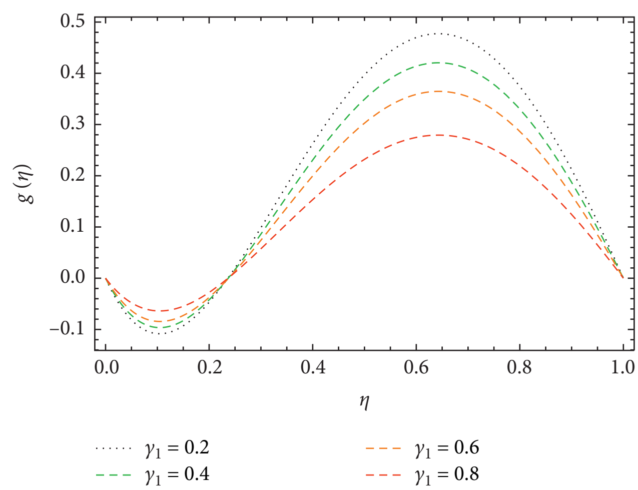

FIGURE 10: Effect of γ_1 on $g(\eta)$ when $R = 0.1, m = 0.8, \beta = 0.4$, and $M = kr = 1$.

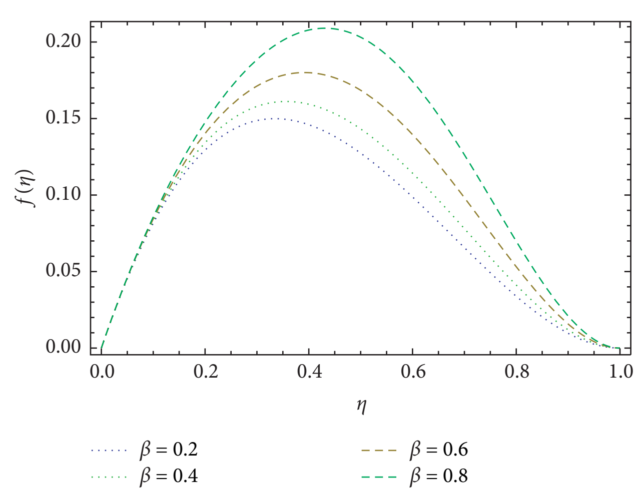

FIGURE 11: Effect of β on $f(\eta)$ when $R = 1, m = \gamma_1 = 0.8, M = 1$, and $kr = 0.6$.

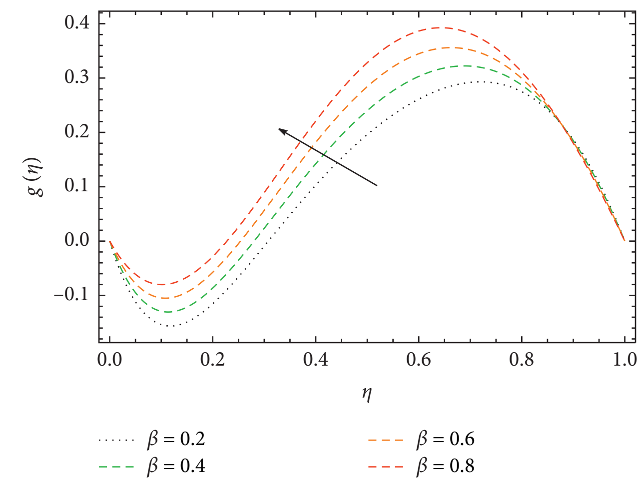

FIGURE 12: Effect of β on $g(\eta)$ when $R = 1, m = \gamma_1 = 0.8, M = 1$, and $kr = 0.6$.

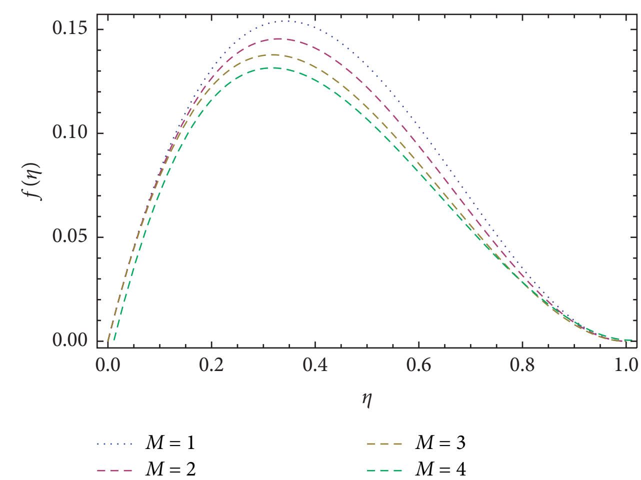

FIGURE 13: Effect of M on $f(\eta)$ and $g(\eta)$ when $R = 1, m = \gamma_1 = 0.8, \beta = 1$, and $kr = 0.6$.

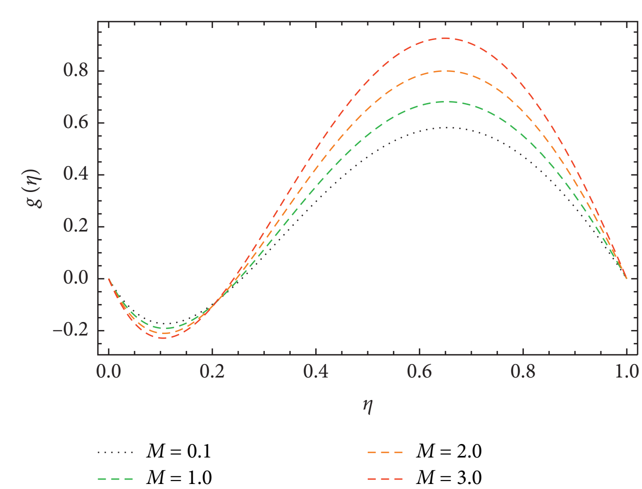

FIGURE 14: Effect of M on $f(\eta)$ and $g(\eta)$ when $R = 1, m = \gamma_1 = 0.8, \beta = 1$, and $kr = 0.6$.

Table 2: Variation in skin friction coefficient for dissimilar values of R, Kr, β, and γ_1 when $m = 0.1$ and $M = 0.5$.

R	Kr	γ_1	β	c_f Shehzad et al. [15] results	c_f Present results
0.01				2.63312	3.86416
0.1	0.5			2.65133	2.94882
0.5		1.0		2.63995	2.64208
	0.0			1.31217	4.33999
	0.5		0.5	1.25917	4.34157
	0.9			1.21694	4.36897
1.0		0.0		2.38508	5.64227
	0.5	0.5		1.25917	5.44576
		0.9		1.03399	4.89911
		1.0	0.0	0.61911	2.22743

$$f_l(\eta) = \frac{1}{l!}\left(\widehat{f}_{\eta}\right)_{q=0},$$
$$g_l(\eta) = \frac{1}{l!}\widehat{g}_{\eta q=0}. \tag{20}$$

3.2. lth-Order Deformation Problem.

$$L_l\left(f_l(\eta) - \prod_l f_{l-1}(\eta)\right) = h_f \mathfrak{R}_l^f(\eta),$$

$$L_{ll}\left(g_l(\eta) - \prod_i g_{l-1}(\eta)\right) = h_g \mathfrak{R}_l^g(\eta),$$

$$\widehat{f}_l = \widehat{f}_l' = \widehat{g}_l = 0, \quad at\ \eta = 0,$$

$$\widehat{f}_l = \widehat{f}' = \widehat{g}_l = 0, \quad at\ \eta = 1,$$

$$\mathfrak{R}_l^f(\eta) = f_{l-1}^{iv} + 2kr g_{l-1} + (1+\gamma_1)\left[R\sum_{j=0}^{l-1}\left(f_{l-1-j}f_j'' - f_{l-1-j}'f_j''\right) - \left(\frac{M}{1} + m^2\right)\left(f_{l-1}'' + mg_{l-1}'\right)\right] \tag{21}$$
$$+ \beta\sum_{j=0}^{l-1}\left(2f_{l-1.-j}''f_j'' - f_{l-1-j.}f_j^{iv} - f_{l-.1-j}'f_{.j}^{v}\right),$$

$$\mathfrak{R}_l^g(\eta) = g_{l-1}'' - (1+\gamma_1)R\sum_{j=0}^{k-1}\left(f_{l-1-j}g_j' - g_{l-1-j}f_j'\right) + Kr \cdot f_{l-1}'$$
$$-\left(\frac{M}{1} + m^2\right)\left(m.f_{l-1}' g_{l-1}\right) + \beta\left(\sum_{j=0}^{l-1} g_{l-1-j}'f_j'' - f_{l-1-j}g_j''\right),$$

where

$$\zeta = \begin{cases} 1, & \text{if } q > 1, \\ 0, & \text{if } q \le 1. \end{cases} \tag{22}$$

4. Convergence of HAM

With the help of assisting constraints h_f and h_g, the convergence region is achieved. The possible region of convergence for the proposed model is given in Figure 2 and Table 1.

5. Results and Discussion

The effect of R on $f(\eta)$ and $g(\eta)$ is given in Figures 3 and 4. An increase in R decreases $f(\eta)$ and $g(\eta)$. The large amounts of viscous energy reduction produce large inertial forces, which decreases $f(\eta)$ and $g(\eta)$. The effect of kr on the $f(\eta)$ and $g(\eta)$ is shown in Figures 5 and 6. It is evident that an increase in kr increases fluid flow due to increase in Cariolis force. This fluid rotation increases kinetic energy which also increases the flow rate. The influence of m and γ_1 on $f(\eta)$ and $g(\eta)$ is given in Figures 7–10, respectively. Both reduce velocity profile. The effect β is given in Figures 11 and 12, showing that the velocity profile increases by increasing β. The relaxation time gets smaller by enhancing γ_1. The effects of M on $f(\eta)$ and $g(\eta)$ are presented in Figures 13 and 14, respectively. β and M oppose the flow due to large relaxation time and magnetic effects. The magnetic field opposes the flow in the y direction and enhance in the z direction.

The numerical values of R, γ_1, β, and kr on C_f are presented in Table 2. We see that C_f has inverse relations with R, γ_1, β and decreases C_f while on direct relation with kr.

6. Conclusion

The following conclusion is observed:

(i) A rise in R causes to decline c_f.
(ii) The mass flux decreases at a lower plate and increases at upper plate.
(iii) R, γ_1, m resist the velocity profile.
(iv) β, Kr assist the velocity profile.
(v) M resists the flow along the y direction and assists the flow along the z direction.

Nomenclature

Gravitational acceleration:	g (m/S^2)
Density:	ρ (kg/m^3)
Distance between two plates:	d (m)
Angular velocity:	Ω (m^2/s)
Magnetic field:	B_0
Ratio of time relaxation to time retardation:	γ_1
Shear stress:	τ (kg/ms^2)
Electrical conductivity:	σ (Siemens per meter (S/m))
Time:	t (S)
Velocity:	V (m/s$_)$
x-component:	u (m/s$_)$
y-component:	v (m/s$_)$
z-component:	w (m/s$_)$
Dynamic viscosity:	μ (kg/ms)
Kinematic viscosity:	ν (m^2/s)
Volume:	V (m^3)
Pressure:	P (N/ m^2).

Data Availability

The data used to support the findings of this study are available in the manuscript.

Conflicts of Interest

The authors declare that they have no conflicts of interest.

References

[1] G. S. Taylor, "Experiments with rotating fluids," *Proceedings of the Royal Society of London*, vol. 100, pp. 114–121, 1921.
[2] H. P. Greenspan, *The Theory of Rotating Fluid*, Cambridge University Press, Cambridge UK, 1968.
[3] S. Goodman, "Radiant-heat transfer between nongray parallel plates," *Journal of Research of the National Bureau of Standards*, vol. 58, p. 2732, 1957.
[4] H. A. Attia and N. A. Kotb, "MHD flow between two parallel plates with heat transfer," *Acta Mechanica*, vol. 117, no. 1–4, pp. 215–220, 1996.
[5] A. K. Borkakoti and A. Bharali, "Hydromagnetic flow and heat transfer between two horizontal plates, the lower plate being a stretching sheet," *Quarterly of Applied Mathematics*, vol. 40, no. 4, pp. 461–467, 1983.
[6] K. Vajravelu and B. V. R. Kumar, "Analytical and numerical solutions of a coupled non-linear system arising in a three-dimensional rotating flow," *International Journal of Non-linear Mechanics*, vol. 39, no. 1, pp. 13–24, 2004.
[7] A. Mehmood and A. Ali, "Analytic solution of three-dimensional viscous flow and heat transfer over a stretching flat surface by homotopy analysis method," *Journal of Heat Transfer*, vol. 130, pp. 121701–121704, 2008.
[8] S. K. Das, U. S. Stephen, W. Y. Choi, and T. Pradeep, *Nanofluids Science and Technology*, Wiley, New York, NY, USA, 2007.
[9] M. S. Tauseef, Z. Ali, K. Z. Khan, and N. Ahmed, "On heat and mass transfer analysis of the flow of a nanofluid between rotating parallel plates," *Aerospace Science and Technology*, vol. 46, pp. 1270–9638, 2015.
[10] H. B. Rokni, D. M. Alsaad, and P. Valipour, "Electrohydrodynamic nanofluid flow and heat transfer between two plates," *Journal of Molecular Liquids*, vol. 216, pp. 583–589, 2016.
[11] T. Hayat, S. Nadeem, and S. Asghar, "Hydromagnetic Couette flow of an Oldroyd-B fluid in a rotating system," *International Journal of Engineering Science*, vol. 42, no. 1, pp. 65–78, 2004.
[12] T. Hayat, K. Muhammad, M. Farooq, and A. Alsaedi, "Squeezed flow subject to Cattaneo-Christov heat flux and rotating frame," *Journal of Molecular Liquids*, vol. 220, pp. 216–222, 2016.
[13] S. Nadeem, M. Sadaf, M. Rashid, and A. S. Muhammad, "Optimal and numerical solutions for an MHD micropolar nanofluid between rotating horizontal parallel plates," *PLoS One*, vol. 6, Article ID 0124016, 2016.
[14] G. B. Jeffrey, "The motion of ellipsoidal particles immersed in a viscous fluid," *Proceedings of the Royal Society of London*, vol. 102, pp. 161–179, 1922.
[15] S. A. Shehzad, T. Hayat, and A. Alsaedi, "MHD flow of Jeffrey nanofluid with convective boundary conditions," *Journal of the Brazilian Society of Mechanical Sciences and Engineering*, vol. 37, no. 3, pp. 873–883, 2014.

[16] S. J. Liao, *The Proposed Homotopy Analysis Method for the Solution of Nonlinear Problems, PhD Thesis*, Shangai Jiao Tong University, Shangai, China, 1992.
[17] S. Liao, "On the homotopy analysis method for nonlinear problems," *Applied Mathematics and Computation*, vol. 147, no. 2, pp. 499–513, 2004.
[18] S. J. Liao, *Homotopy Analysis Method in Nonlinear Differential Equations*, Springer, Berlin, Germany, 2012.
[19] S. Liao, "An optimal homotopy-analysis approach for strongly nonlinear differential equations," *Communications in Nonlinear Science and Numerical Simulation*, vol. 15, no. 8, pp. 2003–2016, 2010.
[20] E. Hall, "On a new action of the magnet on electric currents," *American Journal of Mathematics*, vol. 2, no. 3, pp. 287–292, 1879.
[21] I. Pop and V. M. Soundalgekar, "Effects of Hall current on hydromagnetic flow near a porous plate," *Acta Mechanica*, vol. 20, no. 3-4, pp. 315–318, 1974.
[22] S. Ahmed and J. Zueco, "Modeling of heat and mass transfer in a rotating vertical porous channel with hall current," *Chemical Engineering Communications*, vol. 198, no. 10, pp. 1294–1308, 2011.
[23] A. Riaz, A. Zeeshan, M. M. Bhati, and R. Ellahi, "Peristaltic propulsion of Jeffrey nano-liquid and heat transfer through a symmetrical duct with moving walls in a porous medium," *Physica A: Statistical Mechanics and its Applications*, vol. 545, 2020.
[24] A. riaz, R. Ellahi, S. M. Sait, and T. Muhammad, "Magnetized Jeffrey nanofluid with energy loss in between an annular part of two micro non concentric pipes," *Energy Sources*, 2020.
[25] S. Khan, M. M. Bhati, and A. Riaz, "A revised viscoelastic micropolar nanofluid model with motile micro organismand," *Heat Transfer*, vol. 49, 2020.
[26] A. Wakif, A. Chamkha, T. Thumma, I. L. Animasaun, and R. Sehaqui, "Thermal radiation and surface roughness effects on the thermo-magneto-hydrodynamic stability of alumina–copper oxide hybrid nanofluids utilizing the generalized Buongiorno's nanofluid model," *Journal of Thermal Analysis and Calorimetry*, vol. 143, 2020.
[27] A. Wakif, Z. Boulahia, F. Ali, M. R. Eid, and R. Sehaqui, "Numerical analysis of the unsteady natural convection MHD Couette nanofluid flow in the presence of thermal radiation using single and two-phase nanofluid models for Cu-water nanofluids," *International Journal of Applied and Computational Mathematics*, vol. 4, no. 3, 2018.
[28] M. K. Nayak, A. Wakif, I. L. Animasaun, and M. S. H. Alaoui, "Numerical differential quadrature examination of steady mixed convection nanofluid flows over an isothermal thin needle conveying metallic and metallic oxide nanomaterials: a comparative investigation," *Arabian Journal for Science and Engineering*, vol. 45, no. 7, pp. 5331–5346, 2020.
[29] T. Thumma, A. Wakif, and I. L. Animasaun, "Generalized differential quadrature analysis of unsteady three-dimensional mhd radiating dissipative casson fluid conveying tiny particles," *Heat Transfer*, vol. 49, 2020.
[30] M. Zaydan, A. Wakif, I. L. Animasaun, U. Khan, D. Baleanu, and R. Sehaqui, "Significances of blowing and suction processes on the occurrence of thermo-magneto-convection phenomenon in a narrow nanofluidic medium: a revised Buongiorno's nanofluid model," *Case Studies in Thermal Engineering*, vol. 22, pp. 100726–100732, 2020.
[31] A. Wakif, Z. Boulahia, A. Amine et al., "Magneto convection of alumina water nanofluid within thin horizontal layers using revised generalized Buongiorno's model," *Frontiers in Heat and Mass Transfer*, vol. 12, pp. 3–12, 2019.
[32] M. Fiza, H. Ullah, and S. Islam, "Three-dimensional mhd rotating flow of viscoelastic nanofluid in porous medium between parallel plates," *Journal of Porous Media*, vol. 23, no. 7, pp. 715–729, 2020.